JACS
JOURNAL OF THE AMERICAN CHEMICAL SOCIETY
Article
pubs.acs.org/JACS

Structure and Flexibility of Nanoscale Protein Cages Designed by Symmetric Self-Assembly

Yen-Ting Lai,[†] Kuang-Lei Tsai,[‡] Michael R. Sawaya,[§] Francisco J. Asturias,[‡] and Todd O. Yeates*[,§,∥,#]

[†]Department of Bioengineering, University of California, Los Angeles, California 90095, United States
[‡]Department of Integrative Structural and Computational Biology, The Scripps Research Institute, La Jolla, California 92037, United States
[§]UCLA-DOE Institute for Genomics and Proteomics, University of California, Los Angeles, California 90095, United States
[∥]Department of Chemistry and Biochemistry, University of California, Los Angeles, California 90095, United States
[#]California Nanosystems Institute, University of California, Los Angeles, California 90095, United States

Supporting Information

ABSTRACT: Designing protein molecules that self-assemble into complex architectures is an outstanding goal in the area of nanobiotechnology. One design strategy for doing this involves genetically fusing together two natural proteins, each of which is known to form a simple oligomer on its own (e.g., a dimer or trimer). If two such components can be fused in a geometrically predefined configuration, that designed subunit can, in principle, assemble into highly symmetric architectures. Initial experiments showed that a 12-subunit tetrahedral cage, 16 nm in diameter, could be constructed following such a procedure [Padilla, J. E.; et al. *Proc. Natl. Acad. Sci. U.S.A.* **2001**, *98*, 2217; Lai, Y. T.; et al. *Science* **2012**, *336*, 1129]. Here we characterize multiple crystal structures of protein cages constructed in this way, including cages assembled from two mutant forms of the same basic protein subunit. The flexibilities of the designed assemblies and their deviations from the target model are described, along with implications for further design developments.

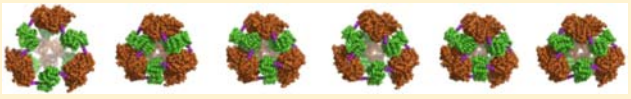

INTRODUCTION

Nature has evolved numerous large and complex molecular structures. These complex structures are often built from protein molecules, with many like-copies assembling together through non-covalent but specific interactions. Viral capsids serve as classic examples, but myriad architecturally sophisticated assemblies exist in nature, including some that are closed or bounded (e.g., clathrin coats, ferritins, vaults, and encapsulins), and others that extend by growth in one or more dimensions (e.g., microtubules, bacterial S-layers, and virus polyhedra).[1] Designing novel protein molecules that can self-assemble to recapitulate such architectures presents a challenging problem in nanobiotechnology.[2,3] Solutions to this problem promise new kinds of biomaterials with diverse applications.

Designing a protein molecule that will assemble into some complex architecture generally requires building at least two distinct kinds of subunit interaction interfaces into the molecule.[4] A number of recent experiments have begun to highlight different strategies for meeting this design requirement.[5−7] Within the last two years, this has resulted in the successful design of novel protein cages, layers, and crystals.[8−12] One method for designing such architectures is to construct the self-assembling protein molecule as a fusion of two distinct protein domains, each of which is known to be naturally oligomeric on its own, so that each of the fused components contributes one of the multiple subunit interfaces required.[5] In order to obtain ordered architectures of predefined types (rather than irregular networks) the two components must be combined in a geometrically defined way according to specific angular rules. A way for doing this was introduced in which the two proteins to be fused are required to have terminal α helices—one protein having its helix at the C-terminus and the other at its N-terminus. Any amino acid residues introduced as a linker between the two fused components must be of the α helix preferring type, with the idea that an unbroken helical connector spanning the two components makes it possible to calculate what the relative geometry between them would be if such a protein was produced experimentally (Scheme 1).[5]

In earlier work, a fusion construct was designed from a trimeric bromoperoxidase enzyme and a dimeric viral matrix protein with nine extra helical residues in the linker. Based on the calculated geometry of the designed construct—i.e., the symmetry axes of the dimer and trimer were nearly intersecting at an angle close to the required angle of 54°—the protein molecule was expected to assemble to form a 12-subunit tetrahedrally shaped cage about 16 nm in diameter. That original construct assembled to form cage-like structures as visualized by electron microscopy, but the resulting material was too heterogeneous to be characterized in atomic detail.[5] Recently, the introduction of a small number of amino acid changes made it possible to crystallize that designed protein assembly; a preliminary structure of one of those variants was

Received: March 4, 2013
Published: April 26, 2013

   dx.doi.org/10.1021/ja402277f | *J. Am. Chem. Soc.* 2013, 135, 7738−7743

Scheme 1. Design of Geometrically Specific Protein Assemblies by Fusing Natural Oligomers through Semi-rigid α-Helical Linkers[a]

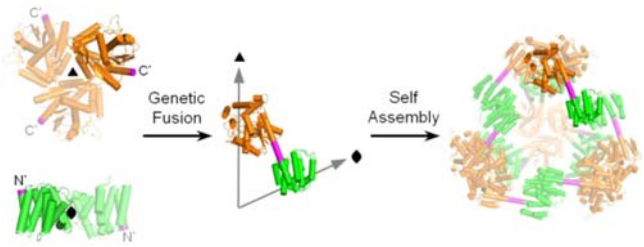

[a]The trimeric domains are colored in orange, the dimeric domains in green, and the helical linkers in magenta.

described earlier.[8] Here, we describe more fully our protein redesign efforts, which have led to a series of variant forms of the designed cage. These variants assemble to form homogeneous, well-ordered structures, which have been elucidated by X-ray crystallography and electron microscopy. Features of flexibility and structural variability in the cages are illuminated.

RESULTS AND DISCUSSION

We hypothesized that the heterogeneous assembly behavior exhibited by our originally designed protein was likely responsible for its failure to crystallize. An idealized molecular model of the fusion protein was created *in silico* to help identify potential design flaws that might have caused the heterogeneity. Upon inspection of the idealized model, residue lysine 118 (Lys118) from the trimeric component of the fusion protein was readily identified as a potential source of steric conflict (Figure S1). When modeled in its native configuration, the closest distance between this residue and the helix linker would have been less than 1 Å (between the Cε atom of the lysine side chain and the Cβ atom of alanine residue 278). Furthermore, none of the common rotamers of lysine could be accommodated at that position without causing spatial conflicts. To fix this structural defect, Lys118 was changed by site-directed mutagenesis to several different amino acids (alanine, serine, leucine, and methionine) to test whether the potentially disruptive interaction between the lysine side-chain and the helix linker could be removed.

When the lysine residue was changed to alanine (Lys118Ala), the solution behavior of the protein was affected dramatically, as revealed by size-exclusion chromatography (SEC) (Figure 1a). The SEC chromatogram of the original design showed a single, asymmetric peak overlapping with the void volume of the size-exclusion column. In contrast, the Lys118Ala mutant showed a dominant major peak corresponding to a molecular weight of ~600 kDa, which was consistent with the intended assembly: 12 subunits of 50.2 kDa each. However, despite extensive crystallization experiments on the major chromatographic fraction, only small, weakly diffracting crystal could be obtained. Further characterization of the Lys118Ala sample by native polyacrylamide gel electrophoresis (PAGE) showed that a heterogeneous population of assembly states was present, though only a single major peak had been discernible on the size-exclusion chromatogram (Figure 1b). An interesting feature evident in the native PAGE gel of the Lys118Ala mutant, but not in the original design, was the presence of discrete, well-separated bands indicating the presence of four

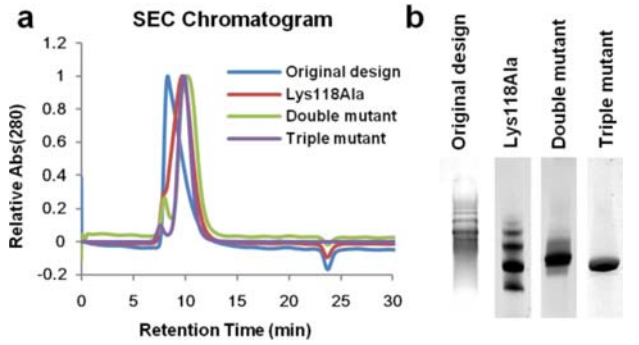

Figure 1. Size-exclusion and native PAGE analysis of designed protein cage mutants. (a) Size-exclusion chromatograms of the different mutants. (b) Native PAGE analysis of the different mutants showed various level of homogeneity. The double mutant is Lys118Ala/Gln24Val. The triple mutant is Lys118Ala/Leu279Gln/Gln24Thr.

specific assembly species in solution. A single mutation from Lys118 to alanine evidently reduced the heterogeneity to a few species, though this was not sufficient to yield well-ordered crystals.

Upon further inspection of the idealized model, we hypothesized that a leucine residue on the helix linker (Leu279) might be the cause of remaining heterogeneity in the single-site Lys118Ala mutant. The hydrophobic leucine side-chain was largely exposed to solvent in the model, and the lack of a stabilizing environment for this side-chain suggested a potentially destabilizing effect on the helix linker. Glutamine 24 (Gln24) on the trimeric domain is located in the spatial vicinity of Leu279, so this position was targeted for mutation to a hydrophobic valine residue to provide a favorable interaction with the side-chain of Leu279 on the linker (Figure S2).

The double mutant Lys118Ala/Gln24Val was characterized by SEC. It showed a dominant peak at an apparent molecular weight close to 600 kDa, which was well-separated from the void peak (Figure 1a). Strikingly, that peak from the SEC showed only a single major band on the native PAGE (Figure 1b), indicating that a homogeneous protein assembly had been obtained. This double mutant was readily crystallized, and structures were determined from two crystal forms, as reported in brief.[8] In these crystal structures, the interdomain linkers adopted helical conformations as intended, and 12 protein subunits assembled into a hollow cage in a tetrahedral arrangement (Figure 2). These structures provided the first clear validation of the helix-based oligomer fusion strategy as a plausible method to create large symmetric protein assemblies.[8] They also revealed surprising deviations from the idealized model and from internal symmetry, as discussed subsequently.

To further test the rationale behind the Gln24Val mutation, which was to provide a favorable (hydrophobic) interaction for Leu279, we created a triple mutant, Lys118Ala/Leu279Gln/Gln24Thr, in order to provide an alternative (polar) contact between residues 24 and 279. This mutant also showed excellent homogeneity by native PAGE (Figure 1b), supporting the conclusion that favorable interactions between the helix linker and the fusion domains are important for homogeneous assembly (Figures S3 and S4).

The triple mutant Lys118Ala/Leu279Gln/Gln24Thr was successfully crystallized and three crystal structures were determined at resolutions of 3.5 Å ($P2_12_12$ space group), 3.6 Å ($P2_12_12_1$ space group) and 7.35 Å ($I222$ space group) (Figure 2 and Table S1). The latter structure was not resolved

dx.doi.org/10.1021/ja402277f | J. Am. Chem. Soc. 2013, 135, 7738−7743

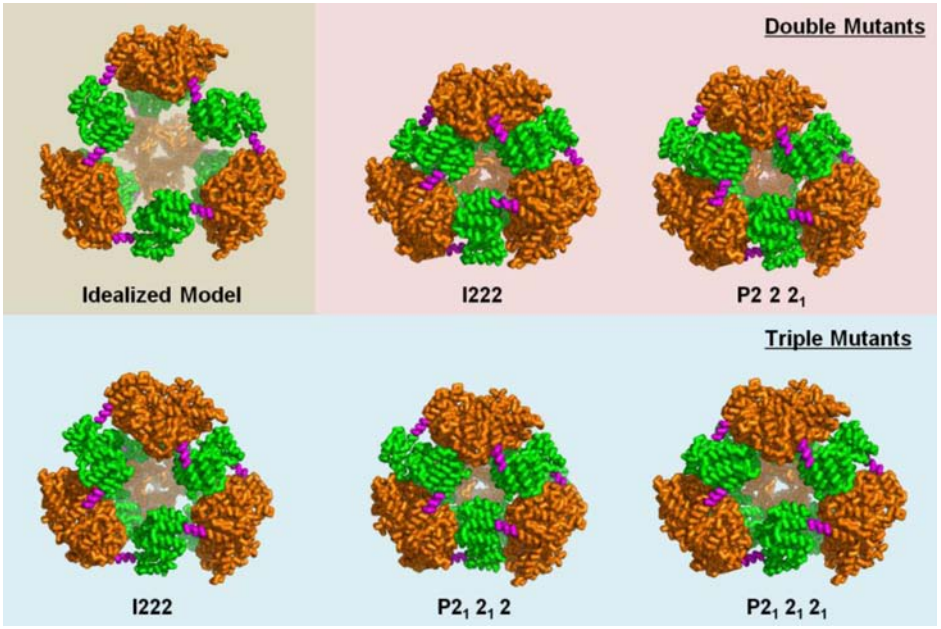

Figure 2. Crystal structures of distinct sequence and conformational forms of a protein cage designed by fusing oligomeric components. The trimeric domains are colored in orange, the dimeric domains in green and the linkers in magenta. A two-amino acid sequence variant and a three-amino acid sequence variant of an initially designed sequence gave cages whose atomic structures could be visualized, in two and three distinct crystal forms, respectively.

in enough detail for full atomic refinement, but the protein domains could be placed without ambiguity. As in the structures of the double mutant, the helix linkers of the triple mutant were clearly visible in electron density maps, including for the lower resolution *I*222 form. The assemblies again formed from 12 protein subunits in a tetrahedral arrangement, as intended. Structures of the triple mutant, like those of the double mutant, showed notable deviations from the ideal model.

Variations among the cage structures were evaluated by superimposing atomic models and by calculating key size parameters. In all cases, the individual protein domains were observed to fold correctly, but essentially rigid-body motions of the domains relative to each other were evident. Among the five structures observed, the *I*222 form of the triple mutant most closely resembles the idealized, symmetric model (Table 1 and Figure S5). In this case, the root-mean-square deviation from the idealized model was 12.8 Å over Cα protein backbone atoms, as calculated by least-squares fitting. While substantial in magnitude, this discrepancy is relatively small in comparison to the size of the entire assembly (169 Å between the two most distant Cα atoms). All five structures suffer from an overall compression, with somewhat different degrees of flattening in different directions. We evaluated the amount of compression by calculating the second central moment mass density distribution ($M_{ij} = \sum_{k\text{-atoms}}(x_{i,k}x_{j,k})/N$) (see eq S1 in the Supporting Information for expanded matrix). Multiplying the eigenvalues of M by three and taking square roots gives the corresponding radii of an elliptical (or spherical) shell (Table 1). The idealized model is cubically symmetric (symmetry group *T*), so its diameters are all equal at 138 Å. The *I*222 crystal structure of the triple mutant is the least compressed overall, though the analysis confirms a distortion of just less than 20% along one direction. Supporting Movie S1 illustrates the rigid body movements that relate the idealized model to the observed *I*222 cage structure of the triple mutant. The deviations between the observed cage structures and the idealized model, and between different instances of the cage structures, prompted further analysis.

Table 1. Structural Deviation of the Cage Mutants from the Idealized Model[a]

	RMS dev. (Å)	Elliptical diameters (Å)	Asymmetry
Model	-	138, 138, 138	0
I222	17.5	121, 112, 103	15%
P222$_1$	17.4	115, 108, 106	8%
I222	12.8	135, 125, 109	19%
P2$_1$2$_1$2	17.6	123, 112, 103	16%
P2$_1$2$_1$2$_1$	16.3	130, 118, 100	23%

[a]The degree of asymmetry was taken as the largest difference between diameters divided by the larger value. The table is color-coded in shades consistent with Figure 2.

We examined the oligomeric interfaces and the helical linkers as potential sources of structural flexibility in the designed cages. The interfaces between the trimeric components of the fusion protein were found to be strictly conserved across all the structures. Experiments also supported the high strength of the native trimeric interaction. The trimer interface appeared to remain intact by SDS-PAGE, as long as the samples were not boiled prior to electrophoresis. The trimer interface could only be disrupted by harsher treatment (e.g., boiling in SDS) or by mutagenesis; after mutating residue 68 at the center of the trimeric interface from threonine to a bulkier glutamine side chain, the trimer interface could be dissociated in SDS without boiling (Figure S6).

dx.doi.org/10.1021/ja402277f | *J. Am. Chem. Soc.* 2013, 135, 7738−7743

In contrast, the dimer interface was seen to be a major source of heterogeneity. Within any given cage structure, some of the dimer interfaces (of which there are six in each cage) were typically found to be in close agreement with the designed model, while some of the dimer interfaces were disrupted (Figure 3a,b). After the choice of oligomeric components for the fusion construct under study here was initially made, subsequent structural studies showed surprisingly that the M1 matrix protein could adopt alternative dimeric configurations.[13] The structures of the designed cages reflect that behavior. It is interesting to note that the dimeric interfaces of the *I*222 structure of the triple mutant are all intact, indicating that, despite the heterogeneous tendencies of the dimeric component, the design could potentially lead to a symmetric cage under some conditions.

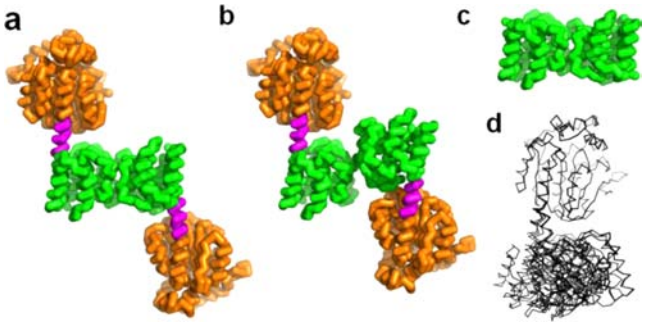

Figure 3. Sources of structural variation in a designed protein cage. (a) The dimeric interface is seen to adopt either the expected, canonical interaction mode, or (b) alternative, apparently weaker, modes of interaction. (c) The canonical interaction mode observed for the natural dimer component in isolation (PDB ID: 1AA7). (d) The six conformationally independent chains of the $P2_12_12$ triple-mutant structure are shown superimposed by their trimeric domains (top). The helix linker and the dimeric domain (bottom) exhibit significant flexibility.

The α-helical linker is another source of variation. The linkers in all the structures retain an essentially helical character, but there are notable deviations, as shown in Figure 3d. These deviations include both bending and twisting motions. The potentially unavoidable flexibility of helical linkers employed in the present strategy has motivated a recent variation on the fusion-based design approach in which a single helical linker is replaced by multiple linkers that may be flexible.[9]

The deviations of the observed crystal structures from the ideal model were initially viewed as a defect of our design. However, these deviations might have unexpected implication in designing dynamic self-assembling protein complexes. For example, in the *I*222 structure of the triple mutant, three protein chains are present in the asymmetric unit, and all the dimeric interfaces are intact, while one helix linker of the three chains is obviously bent. Based on the underlying symmetry, two other energetically equivalent conformations can be constructed by exchanging conformations of the chemically equivalent subunits. The alternation between energetically equivalent states would propagate through the whole cage structure, rendering a surprising range of dynamic motion in the designed assembly (highlighted in Supporting Movie S2). The breakdown of symmetry and the consequent emergence of energetically equivalent states is an important feature in various protein machines, such as rotary ATP synthase and transmembrane antiporters.[14,15] Our finding suggests that it should eventually be possible to design dynamic protein machines intentionally.

To further characterize the individual cage structures in solution (i.e., in the absence of intercage contacts in crystals), we conducted single particle electron microscopy (EM) analysis. (Figure 4). Negative stained EM images showed well-preserved particles, mostly homogeneous in size (Figure 4a). Class averages obtained after alignment and clustering of triple mutant particle images using the ISAC protocol[16] resulted in triangular shaped projections with sides measuring ~15 nm, consistent with the dimensions of the crystal structures (Figure 4b, left). These 2D class averages showed well-defined features that could be matched to projections of the X-ray structures (Figure 4b, right). Some variability in the appearance of ISAC class averages (Figure S7), and matching of specific averages to projections of different crystal forms (Figure 4b), suggest that the triple mutant protein cages are likely to adopt dynamic, partially asymmetric conformations even in a noncrystalline environment, and that the structural flexibility revealed by our different crystal structures reflects an intrinsic property of the cages.

Among the potential applications of artificial protein cages, one is to serve as vectors for biomedical uses. A number of

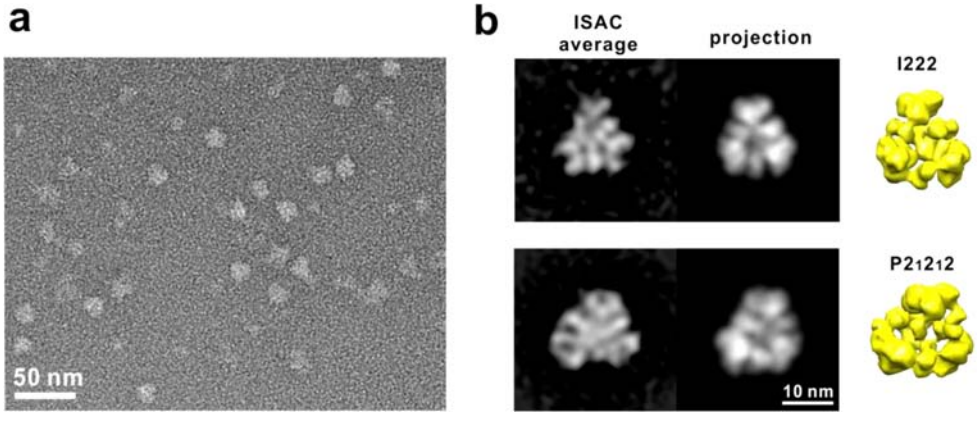

Figure 4. EM analysis of the triple mutant version of the designed protein cage. (a) An EM image showing single particles preserved in uranyl acetate. The scale bar represents 50 nm. (b) 2D class averages (left) obtained after alignment and clustering of cage images, and their correspondence to projections (middle) of volumes generated by low-pass filtration (to 20 Å) of two different X-ray crystal structures of the cage. The scale bar represents 10 nm.

dx.doi.org/10.1021/ja402277f | *J. Am. Chem. Soc.* 2013, 135, 7738−7743

natural protein cages or shells have been tested for various applications, such as drug/gene delivery[17,18] and multivalent antigen display.[19,20] Artificial protein cages aim to expand the available choices for protein containers beyond natural proteins. Because such structures could ultimately provide therapeutic vehicles with novel properties, they represent an area of active investigation.[21−23] For therapeutic and other biomedical applications, protein stability is an important consideration. To test the stability of our artificial protein cage, we used circular dichroism (CD) to monitor thermal denaturation. The CD spectrum confirmed that the protein cage has high α-helical content (Figure S8), consistent with the design and the observed crystal structures. The melting temperature determined from the denaturation curve (based on ellipticity at 222 nm) was ∼58 °C (Figure S8a), which is considerably higher than human body temperature. Interestingly, the protein sample remained clear after heating to 80 °C, and the CD spectrum of the protein sample recovered approximately 70% of its original CD signal after cooling (Figure S8a,b). These preliminary stability studies are encouraging with regard to the potential suitability of these kinds of designed assemblies for future therapeutic developments.

The results of these studies provide a useful perspective on the balance between flexibility and exacting geometric requirements during protein design. The helix-based oligomer fusion approach to designed assembly is combinatorial in nature; it relies on being able to identify a pair of oligomeric protein components of known structure that will have their individual symmetry axes intersecting at some prescribed value (e.g., half the tetrahedral angle of 109.5°), once the two components are connected by a semirigid helical linker of some length. Owing to the discrete nature of the design choices, it is generally not possible to identify components whose construction exactly matches the specified geometric requirements. Indeed, that was the case for the construct that formed the basis for the structural work described here. Based on an assumption of idealized geometry for the helical linker, the symmetry axes of the fused dimer and trimer would have formed an angle of 51.7° (instead of 109.5°/2 = 54.7°). In addition, the two symmetry axes of the hypothetical fusion construct failed to intersect by 6 Å. In order for closed assembly to take place, these model discrepancies must be reconciled somehow. At the outset of these studies, before any crystal structures had been obtained, our expectation was that these relatively small deviations from the target geometry might be accommodated during assembly by small adjustments, like minor flexing, spread throughout the structure. In that scenario, the high symmetry targeted for the assembled structure might be achieved, and the structures obtained might very nearly match the designed model. Instead, the results showed that the response to design imperfections was not spread throughout the structure in the form of minor adjustments, but rather as decisive deviations at a small number of positions. In the present study, those positions were mainly at the dimeric interfaces and the semiflexible helix linkers, which we now recognize to be relatively weak as well as polymorphic.

At present, it is not clear whether the presence of structural deviations at the dimer interfaces should be viewed as a defective outcome arising from a (retrospectively) problematic choice of the dimeric component of the fusion construct, or whether it should be regarded as a feature that allows successful assembly. The combination of a strong interface with a weak interface could be a beneficial feature when the underlying design is not geometrically ideal; deviations at some locations in the structure make it possible for most of the other intended interactions to form. That pattern was evident in the structures observed here. The presence of distinct interfaces with disparate strengths is an important element in systems that show hierarchical assembly.[2,24] Such features are believed to promote reversibility and efficient assembly of correct structures. More insights into these issues should come from further studies of designed structures based on different constructs.

Whatever the source of deviation from symmetry, the observed structures suggest interesting modes of dynamic motion with large amplitudes. Though each crystal structure captures just one perturbation from ideal symmetry, the underlying chemical equivalence of the 12 subunits means that several energetically equivalent ways (12 for the $P2_12_12_1$ structure; six for the $P2_12_12$ structure; three for the $I222$ structure) exist for deforming the structure away from its idealized, symmetric configuration. Animating (or "morphing") between those alternate distortions provides a dramatic perspective into the kinds of dynamic motions likely to be occurring in these cage assemblies in solution (see movies in Supporting Information).

Looking forward, the vast size of the current protein structure database[25] should enable an increasing variety of self-assembling structures to be designed based on the oligomer fusion strategy. Being able to choose from a greater number of building blocks will make it possible to rely on more strongly validated oligomeric components, and to more nearly meet the ideal requirements for symmetric architectures

■ CONCLUSIONS

The present studies further demonstrate the successful use of the helix-based oligomer fusion strategy to design self-assembling protein cages. It is notable however that the successful outcomes relied on an additional cycle of sequence engineering after the initial construct was designed, guided by experimental measures of homogeneity, especially native gel electrophoresis. Also, the cage structures produced so far show notable deviations from the designed models and from perfect internal symmetry. These deviations likely stem from design imperfections related to the limited size of the protein structure database when the design work was begun. With insights gained from recent results, the larger protein structure database[25] and more powerful computer programs for sequence optimization[26,27] should together enable further successes in designing self-assembling protein materials. As this becomes more routine, novel protein materials with useful properties will attract attention as feasible design targets.

■ ASSOCIATED CONTENT

Supporting Information

Full experimental details, supplementary experiments, circular dichroism spectra, 2D class averages from transmission electron microscopy, and animated graphics of protein conformational changes. This material is available free of charge via the Internet at http://pubs.acs.org.

■ AUTHOR INFORMATION

Corresponding Author

yeates@mbi.ucla.edu

Notes

The authors declare the following competing financial interest(s): T.O.Y. is the inventor on a patent held by the University of California on self-assembling proteins.

■ ACKNOWLEDGMENTS

This work was supported by the Biological and Environmental Research program of the Department of Energy Office of Science and by the UCLA MBI Whitcome fellowship to Y.-T.L. Electron microscopy studies were supported by U.S. National Institutes of Health grant R01 67167 (F.J.A.). We thank Duilio Cascio and Michael Thompson for X-ray data collection at the Advanced Photon Source, the staff at APS beamline 24-ID-C, Martin Phillips for assistance with CD spectroscopy, and the National Resource for Automated Macromolecular Microscopy (NRAMM) for support.

■ REFERENCES

(1) Goodsell, D. S.; Olson, A. J. *Annu. Rev. Biophys. Biomol. Struct.* **2000**, *29*, 105.
(2) Zhang, S. *Nat. Biotechnol.* **2003**, *21*, 1171.
(3) Buehler, M. J.; Yung, Y. C. *Nat. Mater.* **2009**, *8*, 175.
(4) Lai, Y. T.; King, N. P.; Yeates, T. O. *Trends Cell. Biol.* **2012**, *22*, 653.
(5) Padilla, J. E.; Colovos, C.; Yeates, T. O. *Proc. Natl. Acad. Sci. U.S.A.* **2001**, *98*, 2217.
(6) Ringler, P.; Schulz, G. E. *Science* **2003**, *302*, 106.
(7) Banappagari, S.; Corti, M.; Pincus, S.; Satyanarayanajois, S. *J. Biomol. Struct. Dyn.* **2012**, *30*, 594.
(8) Lai, Y. T.; Cascio, D.; Yeates, T. O. *Science* **2012**, *336*, 1129.
(9) Sinclair, J. C.; Davies, K. M.; Venien-Bryan, C.; Noble, M. E. M. *Nat. Nanotechnol.* **2011**, *6*, 558.
(10) Brodin, J. D.; Ambroggio, X. I.; Tang, C. Y.; Parent, K. N.; Baker, T. S.; Tezcan, F. A. *Nat. Chem.* **2012**, *4*, 375.
(11) King, N. P.; Sheffler, W.; Sawaya, M. R.; Vollmar, B. S.; Sumida, J. P.; Andre, I.; Gonen, T.; Yeates, T. O.; Baker, D. *Science* **2012**, *336*, 1171.
(12) Lanci, C. J.; MacDermaid, C. M.; Kang, S. G.; Acharya, R.; North, B.; Yang, X.; Qiu, X. J.; DeGrado, W. F.; Saven, J. G. *Proc. Natl. Acad. Sci. U.S.A.* **2012**, *109*, 7304.
(13) Harris, A.; Forouhar, F.; Qiu, S. H.; Sha, B. D.; Luo, M. *Virology* **2001**, *289*, 34.
(14) Yoshida, M.; Muneyuki, E.; Hisabori, T. *Nat. Rev. Mol. Cell. Biol.* **2001**, *2*, 669.
(15) Forrest, L. R. *Science* **2013**, *339*, 399.
(16) Yang, Z.; Fang, J.; Chittuluru, J.; Asturias, F. J.; Penczek, P. A. *Structure* **2012**, *20*, 237.
(17) Buehler, D. C.; Toso, D. B.; Kickhoefer, V. A.; Zhou, Z. H.; Rome, L. H. *Small* **2011**, *7*, 1432.
(18) Lee, L. A.; Wang, Q. *Nanomedicine* **2006**, *2*, 137.
(19) Khor, I. W.; Lin, T. W.; Langedijk, J. P. M.; Johnson, J. E.; Manchester, M. *J. Virol.* **2002**, *76*, 4412.
(20) Paavonen, J.; Jenkins, D.; Bosch, F. X.; Naud, P.; Salmeron, J.; Wheeler, C. M.; Chow, S. N.; Apter, D. L.; Kitchener, H. C.; Castellsague, X.; de Carvalho, N. S.; Skinner, S. R.; Harper, D. M.; Hedrick, J. A.; Jaisamrarn, U.; Limson, G. A. M.; Dionne, M.; Quint, W.; Spiessens, B.; Peeters, P.; Struyf, F.; Wieting, S. L.; Lehtinen, M. O.; Dubin, G. *Lancet* **2007**, *369*, 2161.
(21) Yang, Y. K.; Ringler, P.; Muller, S. A.; Burkhard, P. *J. Struct. Biol.* **2012**, *177*, 168.
(22) Aulisa, L.; Forraz, N.; McGuckin, C.; Hartgerink, J. D. *Acta Biomater.* **2009**, *5*, 842.
(23) Boyle, A. L.; Woolfson, D. N. *Chem. Soc. Rev.* **2011**, *40*, 4295.
(24) Sweeney, B.; Zhang, T.; Schwartz, R. *Biophys. J.* **2008**, *94*, 772.
(25) Berman, H. M.; Coimbatore Narayanan, B.; Costanzo, L. D.; Dutta, S.; Ghosh, S.; Hudson, B. P.; Lawson, C. L.; Peisach, E.; Prlic, A.; Rose, P. W.; Shao, C.; Yang, H.; Young, J.; Zardecki, C. *FEBS Lett.* **2013**, *587*, 1036.
(26) Leaver-Fay, A.; Tyka, M.; Lewis, S. M.; Lange, O. F.; Thompson, J.; Jacak, R.; Kaufman, K.; Renfrew, P. D.; Smith, C. A.; Sheffler, W.; Davis, I. W.; Cooper, S.; Treuille, A.; Mandell, D. J.; Richter, F.; Ban, Y. E.; Fleishman, S. J.; Corn, J. E.; Kim, D. E.; Lyskov, S.; Berrondo, M.; Mentzer, S.; Popovic, Z.; Havranek, J. J.; Karanicolas, J.; Das, R.; Meiler, J.; Kortemme, T.; Gray, J. J.; Kuhlman, B.; Baker, D.; Bradley, P. *Methods Enzymol.* **2011**, *487*, 545.
(27) Allen, B. D.; Mayo, S. L. *J. Comput. Chem.* **2010**, *31*, 904.